Oxygen Abundance in Polar Coronal Holes

L. Teriaca*, G. Poletto*, A. Falchi* and J. G. Doyle†

*Osservatorio Astrofisico di Arcetri, Largo E. Fermi 5, 50125 Firenze, Italy
†Armagh Observatory, College Hill, BT61 9DG Armagh, N. Ireland

Abstract.
Fast solar wind is known to emanate from polar coronal holes. However, only recently attention has been given to the problem of where, *within* coronal holes, fast wind originates. One way to gain information on whether the fast solar wind originates from plumes or interplume regions could consist in comparing the elemental abundances in these regions with the ones characterizing the fast wind. Here we present a first attempt to determine the oxygen abundance in the interplume regions by using spectra taken at times of minimum in the solar cycle (when it is easier to identify these structures) by the SUMER spectrograph aboard SoHO. To this end, we analyze spectra taken in 1996 in polar regions, at altitudes ranging between 1.05 and 1.3 $R_\odot$, finding a value ≥ 8.5 for the oxygen abundance in the interplume regions. From the analysis of the O VI 1032 to 1037 line intensity ratio we also find no evidence of outflow velocities below 1.2 solar radii in interplume regions, while there are indications that outflow motions start to be significant above 1.5 solar radii. The method used and the assumptions made are discussed in light of the derived values. Our values are compared with previous determinations in the corona and solar wind.

INTRODUCTION

Polar coronal holes have long been recognized to be the sources of the high speed solar wind, but only recently it has been identified where, within coronal holes, the solar wind originates. UVCS and SUMER measurements of line widths and of the ratio of the O VI doublet lines at 1032 and 1037 Å in the low corona (at heliocentric distances lower than 2.5 $R_\odot$) seem to indicate that the low density background plasma, rather than the high density plume plasma, is the site where high speed wind originates. Recent analyses of SUMER and UVCS data [see e. g. 1, 2, 3] have shown that the width of UV lines is larger in interplume than in plume regions, hinting to interplumes as the site where energy is preferentially deposited and, possibly, fast wind emanates. Moreover, the [4] analysis of fast polar wind seems to favor the low density regions as sources of the fast wind streams.

A further factor that may differentiate plume and interplume regions is their elemental abundance: a FIP (First Ionization Potential) bias in plumes of ~ 15 has been found by [5]. Because no such factor has been found in fast wind, interplumes most likely do not show such a bias.

Ulysses observations have identified a difference in the elemental abundances of the fast and slow wind: low FIP elements being more enriched, with respect to their photospheric abundance, in the slow speed wind than in the high speed wind. Hence, if interplume regions are really the sources of the fast wind, we may possibly find a different elemental composition between plumes *versus* and interplume plasma at coronal levels.

The purpose of the present work is to shed some light on the plume/interplume composition by determining which oxygen abundance is consistent with the O VI 1032, 1037 Å line intensities, measured in plumes and interplumes, in the range between 1.05 and 1.3 $R_\odot$.

OBSERVATIONS

The observations discussed here were acquired by SUMER on 3 June 1996 and comprise two rasters of the North Polar Coronal Hole (NPCH). The first part consists of a raster scan obtained using the $4'' \times 300''$ slit with an exposure time of 60 s and covering an area of $\sim 278'' \times 300''$ centered at heliocentric coordinates $X = -4''$, $Y = 1150''$. An exposure time of 150 s and the $4'' \times 300''$ slit were used for the second part, covering a region of $\sim 287'' \times 300''$ centered at $X = -6''$, $Y = 1300''$. These rasters were aimed to obtain high signal-to-noise line profiles in the plume and interplume regions above the limb out to 1.5 $R_\odot$.

Data were reduced using various IDL routines from within the SUMER software tree.

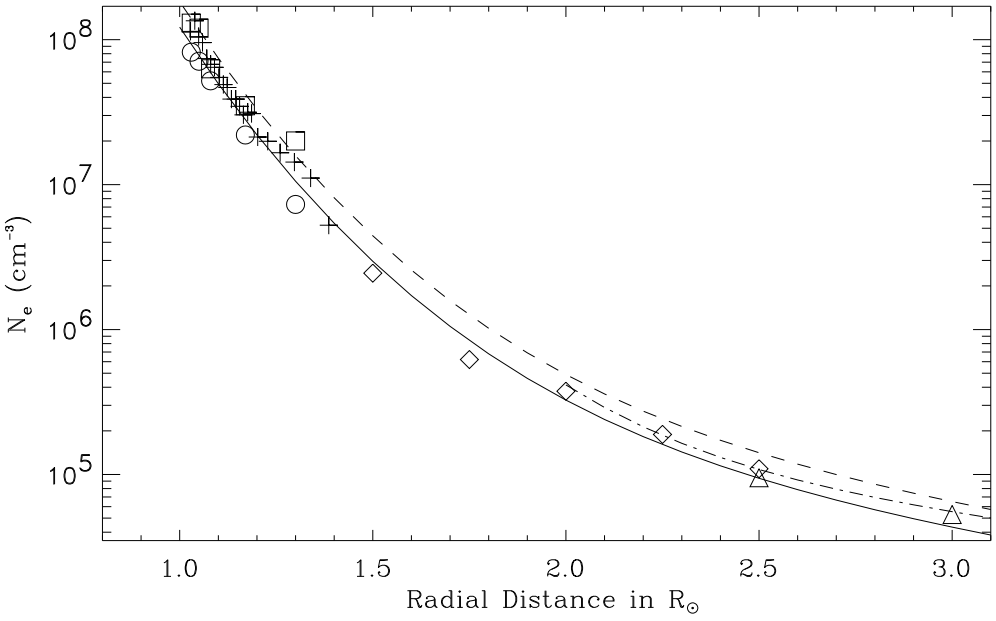

FIGURE 1. Electron density as a function of altitude in polar coronal holes. Measurements obtained in interplume: *crosses* [6], *open squares* [3]. Measurements obtained in plumes: *open circles* [3]. Measurements obtained without distinguishing between plume and interplume: *open diamonds* [7], *open triangles* [8]. Dashed-dotted line shows the expression, valid from 2 to 4 solar radii, given by [9]. Dashed and solid lines represent the adopted density profi les in plumes and interplumes, respectively.

Polar plumes are linear structures that are apparent over the solar poles in visible light, in extreme ultraviolet and in soft X-rays [see 10, and references therein]. Despite the fact that bright plumes are striking features within coronal holes that can extend to more than 30 solar radii from the Sun [10, 11], they only account for a tiny fraction of the solid angle subtended by the polar coronal holes. Plumes are well visible in O VI lines and our rasters show at least three of these structure. After selecting a plume and an interplume region, data within these regions were binned over 5×15 pixels (in the x and y direction, respectively) for the first (lower) scan, and over 4×30 pixels for the second scan. In such a way, line profiles were determined at 15 different locations above the solar limb for both plume and interplume. Further details on this dataset can be find in [2].

DATA ANALYSIS

Spectral profiles were carefully fitted in order to obtain C II 1037, O VI 1032 and O VI 1037 Å line intensities.

Despite the very high quality of the telescope mirror, the level of stray light is not negligible when observations of lines that are bright on disk are carried out above the limb [12, 13].

A chromospheric line, such as C II 1037, can be assumed not to have any coronal contribution and, hence, to be entirely due to stray light. The O VI 1032 stray component at a certain altitude above the limb will be, hence, given by the product of the C II 1037 intensity at that altitude times the ratio of the disk-averaged O VI 1032 and C II 1037 line intensities. The above ratio was evaluated using observations at 1.8 $R_\odot$, were the SUMER spectrum is entirely due to stray light [12, 15, 2].

Errors on line intensities were calculated through Poissonian statistics and, finally, their propagation in the O VI 1032/1037 line ratio was established.

RESULTS AND DISCUSSION

In the case of allowed transitions from the ground level of ions without metastable levels (such as Li-like ions), only the ground level *g* and the excited upper level *u* responsible for the line emission are important for calculating the line intensity and the transition is, hence, well described considering a two level atomic model. This is the case of the O VI 1032 and 1037 Å lines. In the solar corona, these lines are formed by electron impact excitation (collisional component) and by resonant absorption of the O VI radiation from the transition region (radiative

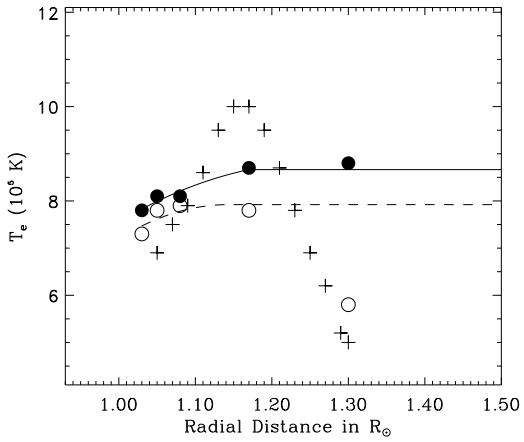

FIGURE 2. Electron temperature as a function of altitude in polar coronal holes. Measurements obtained in interplume (*filled circles*) and plume (*open circles*) regions, respectively [3]. Values obtained without distinguishing between plume and interplume: *crosses* [13]. Dashed and solid lines represent the adopted temperature profi les in plume and interplume, respectively.

component).

$$I_{obs} = I_{Coll.} + I_{Rad.} = 0.85\,\frac{\Delta E_{gu}}{4\pi}\,A_{O/H}\times \times \left[\langle q(T_e)R(T_e)N_e^2\rangle + B_{gu}I_\odot\langle D(T_O,W)R(T_e)N_e\rangle\right] \quad (1)$$

where ΔE_{gu} is the energy of the transition from g to u, $A_{O/H}$ is the oxygen abundance relative to hydrogen, $q(T_e)$ the collisional excitation rate coefficient, B_{gu} is the Einstein absorption coefficient, $I_\odot$ the solar disk's line brightness, $D(T_O,W)$ accounts for Doppler dimming and geometrical dilution factors and is function of the oxygen temperature T_O (consisting of the components parallel and perpendicular to the direction of the magnetic field lines) and the wind velocity W. N_e is the electron number density, $R(T_e)$ is the oxygen ionization fraction calculated in ionization equilibrium and 0.85 is the value of the hydrogen to electron number density ratio as obtained for a fully ionized plasma with composition given by [16]. The quantities in brackets $\langle ...\rangle$ are integrated along the line of sight. Both radiative and collisional components are strongly dependent on the electron density (N_e) and temperature (T_e), and from the oxygen elemental abundance (A_{el}). Hence, in order to obtain information on the abundance through the comparison of observed line intensities with values computed using Eq. 1, we need to know N_e, T_e and W. We are also dealing with the assumption of ionization equilibrium (implied in the calculation of $R(T_e)$) and with the uncertainties in the knowledge of the atomic data (see Raymond *et al.*, present proceedings).

The determination of the electron temperature profile in the solar corona is particularly controversial. The discrepancy between the electron temperatures obtained in the inner corona through spectroscopic diagnostics [see e. g. 3] and the values deduced from ion fractions measurements obtained *in-situ* in the high-speed solar wind by Ulysses [see e. g. 17], is well known. Spectroscopically derived T_e values never exceed 10^6 K in the range 1.05–1.3 $R_\odot$ (see Figure 2). Values by [3] are particularly accurate since they use the ratio of lines of the same ion (Mg IX 706/750), thus avoiding problems with both abundances and differential flow speeds between ions [18]. The closeness in wavelength minimize also the errors arising from the instrument calibration. Moreover, these are the only measurement of T_e in plume and interplume. It has been shown by [18] that in the region 1.05–1.5 $R_\odot$ this ratio is scarcely affected by the presence of a small percentage of electrons following non-Maxwellian distribution functions. From the above discussion we adopted the T_e profiles shown in Figure 2.

The O VI 1032/1037 line ratio is insensitive to T_e [19] and does not depend on the abundance. It is, however, strongly dependent on the electron density N_e as well as on the wind speed W. In order to reproduce the observed line ratio, the N_e profile as a function of height needs to be known, together with the exciting transition region radiation. Densities in coronal holes have been evaluated by several authors [e. g. 9, 20]. However, in the present analysis only data obtained in 1996 (*i. e.* closer in time to our data) were used.

Figure 1 shows N_e as a function of altitude in coronal holes, together with the adopted density profiles in plumes and interplumes. Using those density profiles the O VI 1032 and 1037 line intensities were computed using Eq. 1 and the O VI 1032 to 1037 line ratio was then evaluated. Figure 3 shows that our choice of N_e is able to reproduce the observed line ratios in interplumes with negligible outflow velocity up to 1.3 $R_\odot$. Above this altitude, the comparison with UVCS data obtained on 21 May 1996 in interplume lanes by [4] shows that the region where the fast solar wind is accelerated lies above 1.2 solar radii, as already suggested by [2].

Note that $W \sim 0$, together with the small temperature gradient, implies the assumption of ionization equilibrium being valid at low altitude above the limb. We are, hence, confident in using Eq. 1 for calculating line intensities in the low corona. Using the adopted interplume T_e and N_e profiles, we are able to reproduce the observed intensities in interplumes (Figure 4) with an oxygen abundance of 8.5, which is lower than that measured in the fast solar wind [21]. We note that a higher value of T_e would translate in a higher value of abundance, thus allowing us to consider the value of 8.5 as a lower value of

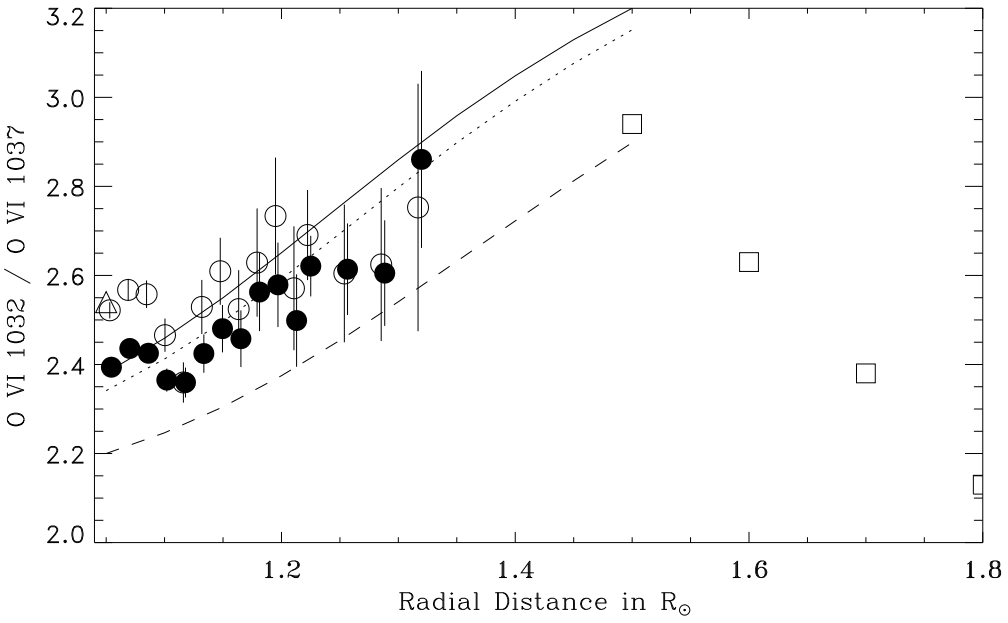

FIGURE 3. O VI 1032 to O VI 1037 intensity line ratios as a function of altitude in polar coronal holes. Values obtained in interplume regions: *open circles* [present paper], *open triangle* [14], *open squares* (UVCS, 21 May 1996) [4]. Values obtained in plumes: *filled circles* [present paper]. Solid and dashed lines represent models for interplume and plume conditions, respectively. Dashed-dotted line represents a mixed model comprising plume and interplume lanes.

the oxygen abundance in the interplume lanes of this polar coronal hole. Similar considerations hold also in the case of the electron density. Higher values of N_e would result in a theoretical ratio *lower* than the observed one, while a lower N_e would result in a small amount of outflow velocity and a higher value of the oxygen abundance.

A realistic attempt to model our plumes observations requires a combination of plume and interplume emissivities along the line of sight, thus introducing an additional free parameter (*i. e.* the plume filling factor). However, it is interesting to note that the introduction of the surrounding interplume plasma is necessary for reproducing the observed line ratios and intensities (see Figures 3 and 5).

CONCLUSIONS

Our measurements of the O VI 1032/1037 line intensity ratio shows that negligible outflow velocities are present below 1.3 $R_o dot$, while an oxygen abundance of 8.5 is required to reproduce the observed O VI line intensities in interplume. This value is lower than the oxygen abundance measured in the fast solar wind. In order to reproduce the abundances measured *in situ*, lower N_e values would be required. Simulations show that densities should be lower by more than a factor two than those adopted. However, such lower N_e profile may imply the solar wind to be accelerated just above ~ 1.2 solar radii. In order to determine the abundances with the above technique, simultaneous determination of electron density, temperature and line intensity are necessary.

ACKNOWLEDGMENTS

L. T. and G. P. are partially supported by MURST. Research at Armagh Observatory is grant-aided by the N. Ireland Dept. of Culture, Arts and Leisure. The SUMER project is financially supported by DLR, CNES, NASA, and PRODEX. SUMER is part of SoHO, the Solar and Heliospheric Observatory of ESA and NASA.

REFERENCES

1. Giordano, S., Antonucci, E., Noci, G., and *others*, *Astrophysical Journal*, **531**, L79–L82 (2000).
2. Banerjee, D., Teriaca, L., Doyle, J. G., and Lemaire, P., *Solar Physics*, **194**, 43–58 (2000).
3. Wilhelm, K., Marsch, E., Dwivedi, B. N., and *others*, *Astrophysical Journal*, **500**, 1023–1038 (1998).

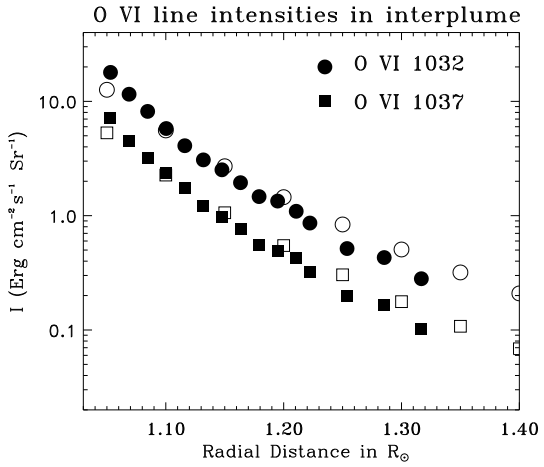

FIGURE 4. O VI line intensities as a function of altitude in an interplume region of the North polar coronal hole. Filled circles and squares represent the O VI 1032 and O VI 1037 observed line intensities. Open circles and squares represent the O VI 1032 and O VI 1037 modeled line intensities for the adopted interplume conditions.

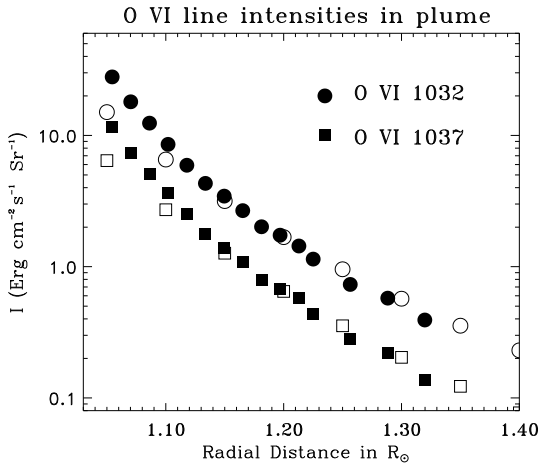

FIGURE 5. O VI line intensities as a function of altitude in a plume region of the North polar coronal hole. Filled circles and squares represent the O VI 1032 and O VI 1037 observed line intensities. Open circles and squares represent the O VI 1032 and O VI 1037 modeled line intensities obtained by combining plume and interplume models.

4. Antonucci, E., Dodero, M. A., and Giordano, S., *Solar Physics*, **197**, 115–134 (2000).
5. Widing, K. G., and Feldman, U., *Astrophysical Journal*, **392**, 715–721 (1992).
6. Doyle, J. G., Teriaca, L., and Banerjee, D., *Astronomy and Astrophysics*, **349**, 956–960 (1999).
7. Zangrilli, L., Private communication (2001), unpublished.
8. Lamy, P., Quemerais, E., Liebaria, A., and *others*, "Electronic Densities in Coronal Holes from LASCO-C2 Images", in *Fifth SOHO Workshop: The Corona and Solar Wind Near Minimum Activity*, edited by A. Wilson, ESA SP 404, ESA Publications Division, ESTEC, Noordwijk, The Netherlands, 1997, pp. 491–494.
9. Kohl, J. L., Noci, G., Antonucci, E., and *others*, *Astrophysical Journal*, **501**, L127–L131 (1998).
10. DeForest, C. E., Hoeksema, J. T., Gurman, J. B., and *others*, *Solar Physics*, **175**, 393–410 (1997).
11. DeForest, C. E., Plunkett, S. P., and Andrews, M. D., *Astrophysical Journal*, **546**, 569–575 (2001).
12. Lemaire, P., Wilhelm, K., Curdt, W., and *others*, *Solar Physics*, **170**, 105–122 (1997).
13. David, C., Gabriel, A. H., Bely-Dubau, F., and *others*, *Astronomy and Astrophysics*, **336**, L90–L94 (1998).
14. Patsourakos, S., and Vial, J. C., *Astronomy and Astrophysics*, **359**, L1–L4 (2000).
15. Hassler, D. M., Wilhelm, K., Lemaire, P., and Schüle, U., *Solar Physics*, **175**, 375–391 (1997).
16. Feldman, U., Mandelbaum, P., Seely, J. F., and *others*, *Astrophysical Journal Supplement*, **81**, 387–408 (1992).
17. Ko, Y. K., Fisk, L. A., Geiss, J., and *others*, *Solar Physics*, **171**, 345–361 (1997).
18. Esser, R., and Edgar, R. J., *Astrophysical Journal*, **532**, L71–L74 (2000).
19. Li, X., Habbal, S. R., Kohl, J. L., and Noci, G., *Astrophysical Journal*, **501**, L133–L137 (1998).
20. Fisher, R., and Guhathakurta, M., *Astrophysical Journal*, **447**, L139–L142 (1995).
21. von Steiger, R., Fisk, L. A., Gloeckler, G., and *others*, "Composition Variations in Fast Solar Wind Streams", in *Solar Wind Nine, Proceedings of the Ninth International Solar Wind Conference*, edited by S. R. Habbal, R. Esser, J. V. Hollweg, and P. A. Isenberg, AIP Conference Proceedings 471, American Institute of Physics, New York, 1999, pp. 143–149.